Load Relief Control System for Launch Vehicle based on Acceleration Feedback

Josy John
(Department of Electrical Engineering, College of Engineering Trivandrum, India)

Abstract: *Launch vehicle experience significant disturbance moment in the atmospheric phase. During the high dynamic pressure region, wind causes additional angle of attack increasing the aerodynamic and structural load. Classical attitude control based on angular position and rate feedback minimize trajectory dispersions and provide minimal load reduction. Load relief system is used to minimize the aerodynamic load with acceptable trajectory dispersion. This paper deals with classical attitude control and load relief control based on acceleration feedback. Control gains are designed by pole placement method considering rigid body dynamics. Flexible dynamics is also considered and separate filter is designed for both cases to satisfy the rigid and flexible margins. The load relief effect of both cases is examined in the presence of wind.*
Keywords: *Attitude Control, Flexible Dynamics, Load Relief Control, Pole Placement method, Rigid body Dynamics.*

I. Introduction

The primary objective of a launch vehicle control system is to stabilize the vehicle during flight in presence of various disturbing forces and moments and to make the vehicle follow the steering commands. Conventional attitude control system based on drift minimum control uses angular position and rate feedback to minimize the trajectory dispersions. Drift minimum control may not meet the requirements of allowable load limits in presence of wind disturbance [1], [2]. The control system must be concerned with loads resulting from forces such as atmospheric force, propulsive force, aerodynamic force etc. These forces along with angle of attack causes structural load. The vehicle structure determines the allowable load limit and bending moments. The major disturbance to the launch vehicle during the high dynamic pressure period is the in-flight winds, and it causes extra aerodynamic load due to the wind induced angle of attack. Load relief system is used to decrease the aerodynamic load by reducing the angle of attack [3], [4].

Load relief techniques are of two types- active and passive. The passive load relief technique highly relies on the accuracy of the preinstalled wind data. Passive systems for load reduction rely on balloon wind measurement systems, such as jimsphere or rawindsonde balloons, to determine the wind speed and direction at high altitudes. The movement or drift of the balloon is generally measured with a ground based radar tracking system. These wind measurement systems do not measure the wind speed and direction along the actual expected flight path of the vehicle due to the associated wind drift of the balloons. Since wind speed and direction are constantly changing, the actual winds experienced by the launch vehicle during flight can be significantly different from those measured prior to flight [5]. Thus research in active technology has gained more attention. Active load relief method uses feedback based on angle of attack, acceleration etc. to reduce the aerodynamic load. The flight control system is designed with an active load relief feedback loop for the launch vehicle to reduce the airframe loading in the high dynamic pressure period of flight when wind velocities produce the largest vehicle bending moments. The time of usage is dependent on the selected control law. Control law properties range from those which produce large load relief coupled with large trajectory dispersions to those which minimize trajectory dispersions and produce minimal load relief [6]. In this paper, load relief control system based on acceleration feedback is analyzed at high dynamic pressure period and compared with classical attitude control system. Pole placement method is used to design the control gain values. Both rigid body dynamics and flexible dynamics of the system is studied and suitable filter to satisfy performance margin is designed. Performance of load relief system in presence of wind disturbance is examined and compared with the classical attitude control system.

II. Mathematical Modelling

Attitude control system of launch vehicle is analyzed using the short period dynamics. Different assumptions used for developing the dynamics are time slice approach, small angle approximation, decoupling of attitude dynamics and neglected non-linearities. All above assumptions lead to Linear Time Invariant (LTI) properties of the system. Both rigid body and flexible body motion is expressed as short period dynamics.
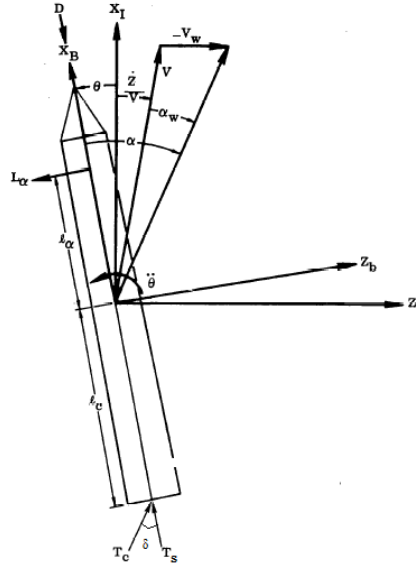
Fig. 1 Geometry of launch vehicle in pitch plane

2.1 Rigid Body Dynamics

The schematic diagram of a launch vehicle geometry in pitch plane is given in Fig. 1. A right hand coordinate system where the X axis is along the vertical axis and Z axis along the horizontal direction is assumed. Body fixed reference frame (X_B, Y_B, Z_B) which is fixed to the vehicle such that origin is located at the vehicle geometric centre. The motion will be described with reference to an inertial coordinate system (X_I, Y_I, Z_I) [2]. Let θ be the attitude angle and V be the relative velocity vector of the vehicle. The force acting on Z direction in terms of normal and axial force components can be written as

$$m\ddot{Z} = (T_T - D)\cos(90 + \theta) + T_c\cos(\theta) - L_\alpha \alpha \cos\theta \qquad (1)$$

where m is mass of the vehicle, θ is the pitch attitude angle, L_α is Aerodynamic lift force acting on the system per unit angle of attack, T_T is total thrust force, D is axial force acting on the system, δ is engine deflection angle and T_c is control torque. For thrust vector control of launch vehicle, thrust vector is deflected by an angle δ giving control thrust. By small angle approximation (1) becomes

$$m\ddot{Z} = -(T_T - D)\theta + T_c - L_\alpha \alpha \qquad (2)$$

where $T_c = K_{ds}\delta$ and K_{ds} is the side force per unit pintle deflection. Secondary Injection Thrust Vector Control is considered. Thus (2) can be written as

$$\frac{\ddot{Z}}{V} = -\frac{(T_T - D)}{mV}\theta + \frac{K_{ds}}{mV}\delta - \frac{L_\alpha}{mV}\alpha \qquad (3)$$

Sum of moments caused by thrust and lift force gives the total moment acting about center of gravity of the system as

$$I_{yy}\ddot{\theta} = T_c l_c \delta + L_\alpha l_\alpha \alpha \qquad (4)$$

$$\ddot{\theta} = \mu_c \delta + \mu_\alpha \alpha \qquad (5)$$

where $\mu_\alpha = \dfrac{L_\alpha l_\alpha}{I_{yy}}$ is aerodynamic moment coefficient and $\mu_c = \dfrac{K_{ds} l_c}{I_{yy}}$ is the control moment coefficient, l_α is the distance from centre of pressure to origin of body axis in pitch plane, l_c distance from origin of body axis system to engine swivel point and I_{yy} is the moment of inertia about pitch axis.

$\dot{Z}$ is the inertial drift velocity and $\dfrac{\dot{Z}}{V}$ gives the angle of attack due to drift. Resultant of relative vehicle velocity and wind velocity will give the effective wind velocity vector. The angle between body axis and the resultant velocity vector gives the total angle of attack. Thus angle of attack, α is the vector sum of three angles.

$$\alpha = \theta + \frac{\dot{Z}}{V} + \alpha_w \qquad (6)$$

where α_w is angle of attack due to wind and is given by $\alpha_w = -\dfrac{V_w}{V}$.

Equation for lateral acceleration as can be written as

$$a_s = \ddot{Z}_b - l_m \ddot{\theta} \tag{7}$$

where l_m is the distance of accelerometer to centre of gravity.

The transfer functions for $\dfrac{\theta(s)}{\delta(s)}$ and $\dfrac{a_s(s)}{\delta(s)}$ according to the above rigid body equations of motions can be derived as

$$\frac{\theta(s)}{\delta(s)} = \frac{\mu_c\, s + c_2}{s^3 + d_1\, s^2 - \mu_\alpha\, s + \mu_\alpha c_1} \tag{8}$$

$$\frac{a_s(s)}{\delta(s)} = \frac{a_1\, s^3 + a_2\, s^2 + a_3\, s + a_4 c_1}{s^3 + d_1\, s^2 - \mu_\alpha\, s + \mu_\alpha c_1} \tag{9}$$

where

$$c_1 = \frac{T_T - D}{mV}, \quad d_1 = \frac{L_\alpha}{mV}, \quad d_2 = \frac{K_{ds}}{mV}, \quad c_2 = d_1 \mu_c + d_2 \mu_\alpha$$

$$a_1 = \frac{K_{ds}}{m} - \mu_c l_m, \qquad\qquad a_2 = \left(-\frac{L_\alpha}{mV} - \mu_\alpha l_m\right)\frac{K_{ds}}{mV} + \left(\frac{K_{ds}}{m} - \mu_c l_m\right)\frac{L_\alpha}{mV},$$

$$a_3 = \left(-\frac{L_\alpha}{m} - \mu_\alpha l_m\right)\mu_c - \left(\frac{K_{ds}}{m} - \mu_c l_m\right)\mu_\alpha, \quad a4 = \frac{T_T - D}{mV}\left[\left(\frac{L_\alpha}{m} + \mu_\alpha l_m\right)\mu_c + \left(\frac{K_{ds}}{m} - \mu_c l_m\right)\mu_\alpha\right] \tag{10}$$

2.2 Flexible Body Dynamics

The satisfactory performance of an autopilot controlled flexible launch vehicle depends on the accurate representation of the vehicle's elastic motion under prescribed forces. This due to the fact that the forces and moments applied by propulsion device relies on the output from the sensors. This output include signals representing both the rigid body motions and local elastic distortions. Therefore under adverse conditions, the autopilot will act to reinforce the amplitudes of oscillations leading ultimately to structural failure of vehicle. The elastic deflections are represented in terms of free modes of vibration of the system [2]. The elastic deflection at any point along the vehicle is given as

$$\xi(l,t) = \sum_{i=1}^{n} q^{(i)}(t)\phi^{(i)}(l) \tag{11}$$

where $\xi(l,t)$ is bending deflection in pitch plane, $q^{(i)}(t)$ is generalised co-ordinate of ith bending mode and $\phi^{(i)}(l)$ is the normalised mode shape of ith bending mode. This satisfies the bending equation given below

$$\ddot{q}^{(i)} + 2\zeta^{(i)}\omega^{(i)}\dot{q}^{(i)} + [\omega^{(i)}]^2 q^{(i)} = -\frac{Q^{(i)}}{M^{(i)}} \tag{12}$$

where $Q^{(i)} = \int_0^L F_z \phi^{(i)}(l)\ dl$ is the generalised force for the ith bending mode and $M^{(i)}(l) = \int_0^L m(l)\left[\phi^{(i)}(l)\right]^2 dl$ is the generalised mass for i^{th} bending mode. $\sum F_z$ is the normal force on the vehicle and $m(l)$ is the reduced mass per unit length along longitudinal axis of vehicle.

In load relief system, three sensors are required- position gyro, rate gyro and accelerometer. The output of these sensors can be thus obtained as

Position Gyro Output

$$\theta_P = \theta + \sum_{1}^{n} \sigma^{(i)}(l)q^{(i)} \tag{13}$$

Rate Gyro Output

$$\theta_R = \dot{\theta} + \sum_{1}^{n} \sigma^{(i)}(l)\dot{q}^{(i)} \tag{14}$$

Accelerometer Output

$$a_{sf} = a_s - \sum_{1}^{n} \frac{T_T}{m}\sigma^{(i)}(l_t)q^{(i)} + \phi^{(i)}(l_a)\ddot{q}^{(i)} - U_0\sigma^{(i)}(l_a)q^{(i)} \tag{15}$$

where $\sigma^{(i)}(l) = -\dfrac{\partial\phi^{(i)}(l)}{\partial l}$ is the negative slope for ith bending mode at the sensor location. l_t and l_a indicates the thrust location and accelerometer location.

III. Controller Design

The conventional attitude control law is modified by incorporating acceleration feedback loop in order to attain the load relief feature. Thus the load relief control law is obtained as

$$\delta = -K_A(K_\theta[\theta_c - \theta] + K_R\dot{\theta} + K_z a_s) \qquad (16)$$

where K_A is the forward gain K_θ is the position gyro gain, K_R is the rate gyro gain and K_z is the accelerometer gain.

The control gain values are designed using pole placement method to obtain required specifications. The design is carried out at regular interval of time during a flight trajectory and the gains schedule is thus arrived. The design specifications (rigid body and actuator specifications) can be transformed into desired pole locations in s-plane. Gain values are computed by equating the coefficients of like powers in system characteristic equation and the desired characteristic equation [7]. The advantage of this method is that we will get closed form expressions for gains as function of vehicle parameters and placed poles. The load relief control is attempted at high dynamic pressure region where the winds become potentially dangerous i.e. from 40 to 70 seconds of flight time. Conventional attitude control is applied during remaining time. This provides accurate control consistent with the structural strength of vehicle [4].

3.1 Rigid Body Design
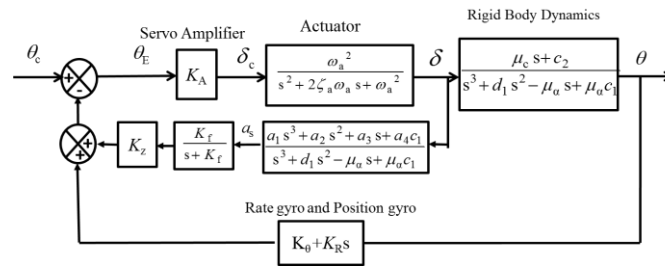
Fig. 2 Block diagram of rigid body load relief control

Fig. 2 shows the load relief control system with acceleration feedback loop. Attitude control is obtained when this loop is opened i.e. $K_z = 0$ and K_θ is set equal to 1. The gain values of both attitude controller and load relief controller are calculated using pole placement method. Rigid body dynamics is considered while calculating gain values. Desired pole locations include the rigid body poles, actuator poles and drift pole. One additional accelerometer pole comes when load relief feature is employed. Rigid body natural frequency ω_n is taken as 4 rad/s and damping ratio, ζ_n as 0.8. Actuator natural frequency, ω_a is taken as 4.5Hz and damping ratio, ζ_a as 0.707. Second order sensor dynamics is assumed with natural frequency, $\omega_s = 17.5$Hz and damping ratio, $\zeta_s = 0.707$. The desired margins for rigid body dynamics are Aero Margin (AM) and Gain Margin (GM)>6dB and Phase Margin (PM)>30°.

3.1.1 Attitude Control: For attitude control, the desired poles are taken as $-p$, $-a \pm jb$ and $-\zeta_n\omega_n \pm j\omega_n\sqrt{1-\zeta_n^2}$ to obtain a fifth order desired characteristic equation. The gain values K_A and K_R calculated for 100s flight time is shown in Fig. 3.
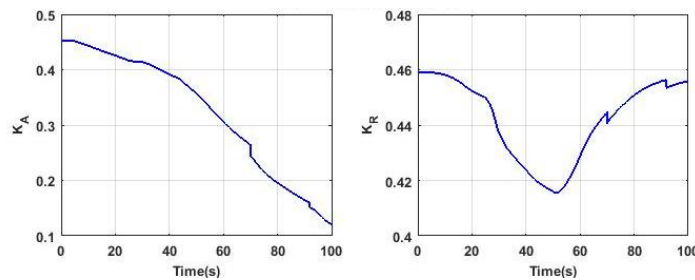
Fig. 3 Gain values for attitude control

At T=Ignition+ 50s the gain values obtained with attitude control are K_A =0.3562, K_R =0.4156 and K_θ =1. The performance with designed gain value is evaluated by taking Bode and Nyquist plots. The rigid body attitude control design yields sufficient margins of AM=18.3dB, GM=13.2dB and PM=46.2°. At all-time instants, the margins are found to be satisfied.

3.1.2 *Load Relief Control*: In load relief control, the desired closed loop poles taken are $-p_1$, $-p_2$, $-p_3$ and $-\zeta_n \omega_n \pm j \omega_n \sqrt{1-\zeta_n^2}$. An accelerometer filter $\dfrac{K_f}{s + K_f}$ with K_f =3 is used for filtering the acceleration signal so as to provide a smooth signal. The drift pole is assumed at -0.01 in the s-plane. For the easy analysis, equivalent first order actuator $\dfrac{K_c}{s + K_c}$ with K_c =19 is assumed while derivation. Thus a fifth order system characteristic equation is obtained with equivalent first order actuator. For all other analysis, second order actuator is assumed. The control gain values computed are as shown in Fig. 4.
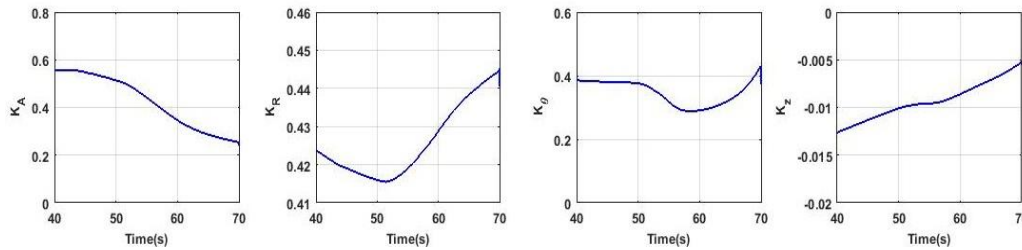
Fig. 4 Gain values for load relief control

At T=Ignition+ 50s, the gain values obtained using load relief control are K_A =0.5137, K_θ =0.3758, K_R =0.4160 and K_z = -0.0101. The margins obtained with rigid body load relief control design are AM=19.8dB, GM=11.7dB and PM=45°. At 50s and for all time instants the margins are satisfied.

3.2 Flexible Body Design

Flexible dynamics is included in the system by introducing first two bending modes. With inclusion of flexibility, the Bending Mode lag Phase Margin (BMPM) should be greater than 60°. When analyzing the frequency response plots of controlled system, it is identified that the desired performance specifications are not met when flexibility is introduced. In order to achieve sufficient margins, filter has to be designed for both attitude control and load relief control.

3.2.1 *Attitude Control:* Lag-lead compensator C is designed for 0 to 40s, 40 to 70s and 70 to 100s as 3 intervals of flight time to achieve the rigid body and flexible margins.

For 0 to 40s:
$$C = 0.987 \left(\frac{0.3964s + 1}{0.0556s + 1} \right) \left(\frac{0.3333s + 1}{1.6385s + 1} \right) \tag{17}$$

For 40s to 70s:
$$C = \left(\frac{0.3843s + 1}{0.0425s + 1} \right) \left(\frac{0.3325s + 1}{1.7292s + 1} \right) \tag{18}$$

For 70 to 100s:
$$C = \left(\frac{1.0977s + 1}{0.0071s + 1} \right) \left(\frac{0.3828s + 1}{6.8068s + 1} \right) \tag{19}$$
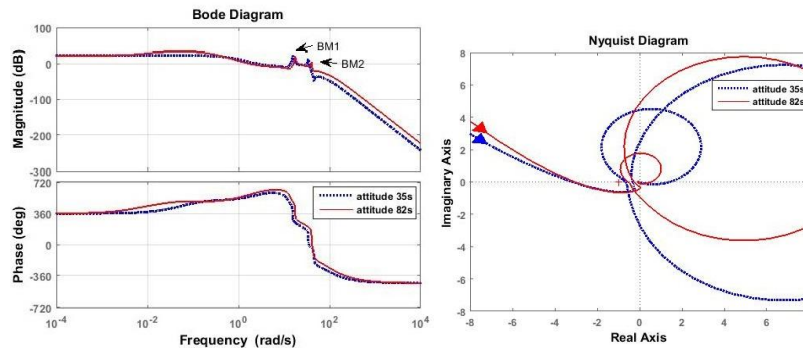
Fig. 5 Bode and Nyquist plot of compensated attitude control system

The Bode and Nyquist plots of compensated system at 35s and 82s is as shown in Fig. 5. The margins of compensated system at 35s are AM=10.1dB, GM=9.33dB, PM=38.7°, BMPM=60.2° and at 82s are AM=9.77dB, GM=11.7dB, PM=41.5°, BMPM=93.3°. Thus all margins are satisfactory with designed compensator at both time instants.

3.2.2 Load Relief Control: Due to acceleration feedback the bending mode peaks have gone up. So notch filter is required to attenuate the bending mode peaks for gain stabilisation. Notch filter, N is designed for a depth of 30dB. Further a lag-lead compensator, C is designed to satisfy the rigid body and flexible margins.

For 40 to 70

$$C = 0.6875 \left(\frac{0.44s + 1}{0.0957s + 1} \right) \left(\frac{1.4s + 1}{3.1362s + 1} \right) \tag{20}$$

$$N = \left(\frac{0.003844s^2 + 0.0028s + 1}{0.003844s^2 + 0.089s + 1} \right) \tag{21}$$
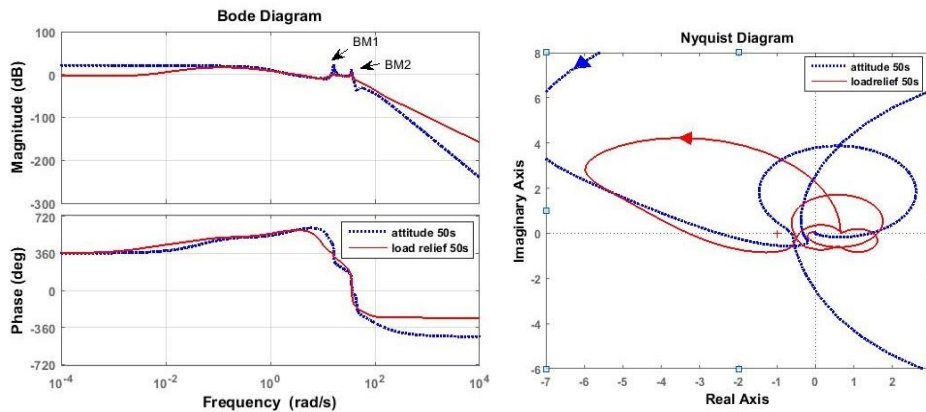
Fig. 6 Bode and Nyquist plot of compensated attitude and load relief control system at 50s

The Bode and Nyquist plots of compensated load relief system along with compensated attitude control system at 50s is as shown in Fig. 6. The compensated system with notch filter and lag-lead compensator provides acceptable margins of AM=10.4dB, GM=7.64dB, PM=44.5° and BMPM=137° at 50s. Pure attitude control at 50s yields AM=8.01dB, GM=9.86dB, PM=34.4° and BMPM=60.8°.

IV. Results and Discussion

The filters designed for both attitude control and load relief control is found to provide sufficient stability margins. The margins obtained for different time instants is as shown in Fig. 7.
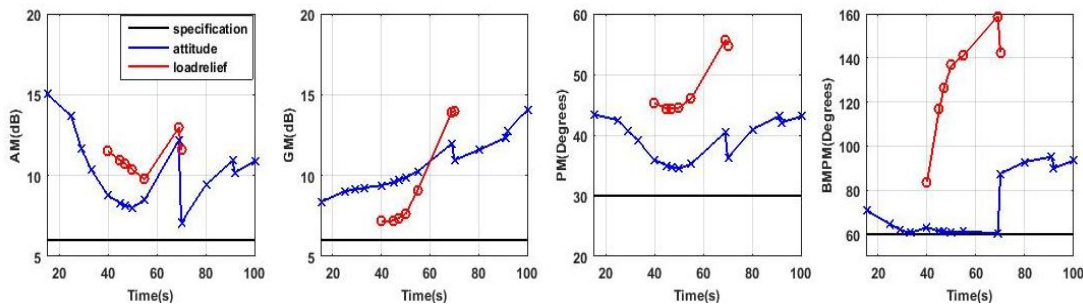
Fig. 7 Margins of compensated system with attitude control and load relief control

Time domain analysis of the system with attitude controller and load relief controller is carried out by analysing the step response of system. The response of both systems with unit step reference attitude at 50s is shown in Fig. 8. The attitude controller yields an overshoot of 33.7 % and an attitude error of 0.02° which satisfies the required specification of overshoot<35% and attitude error<1° during attitude control. The attitude error should be less than 3° when the load relief controller is employed. The attitude error obtained with load relief controller at 50s is 0.38° which is well within the limits. It's clear from the response that trajectory dispersion is more compared to attitude control. This is due to the fact that lateral drift during load relief control is more since the vehicle is turned into wind to decrease the lateral forces.
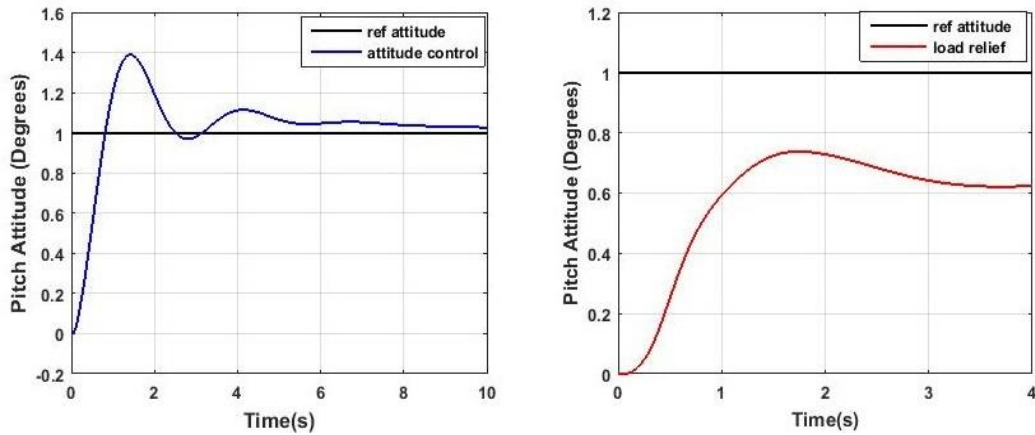
Fig. 8 Step response of attitude control and load relief control system at 50s
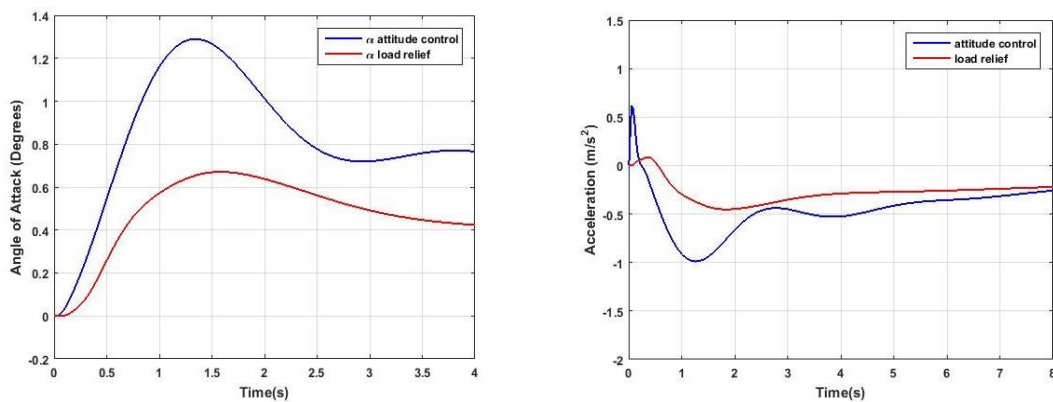
Fig. 9 Angle of attack and acceleration response to unit step attitude at 50s

The angle of attack and acceleration responses with unit step reference attitude are also shown in Fig. 9. It is clear from the responses, that attitude control gives higher values of angle of attack and acceleration. Both angle of attack and acceleration can be considered as a measure of load acting on the system.These responses indicates that load relief controller achieves better load reduction compared to the classical attitude controller.
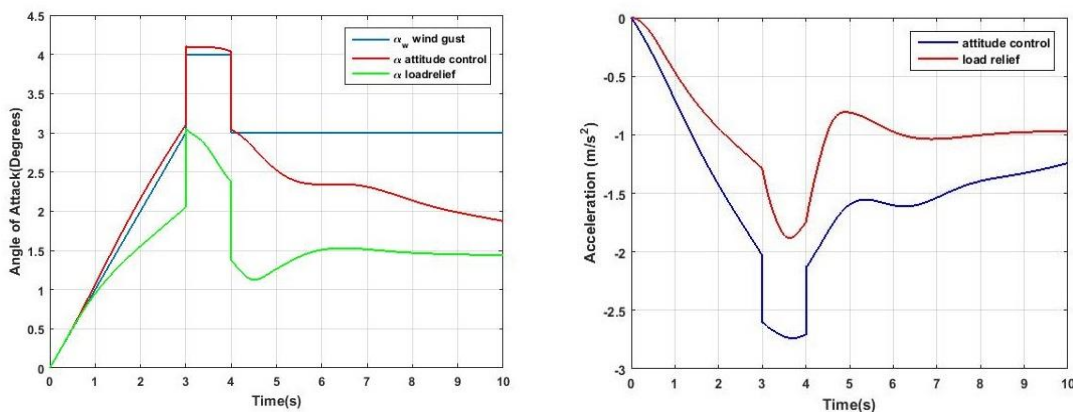
Fig. 10 Angle of attack and acceleration response of attitude control and load relief control system with positive wind gust

The response of the system with a positive and negative wind gust is analysed to check for the load reduction capability of designed system in presence of wind disturbance. The positive and negative wind gust responses are shown in Fig. 10 and Fig. 11.
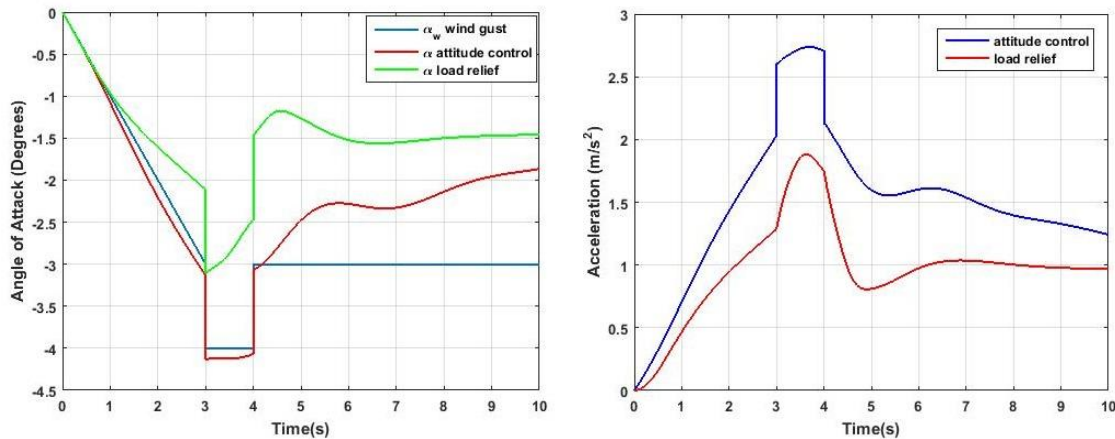
Fig. 11 Angle of attack and acceleration response of attitude control and load relief control system with negative wind gust

In case of attitude control, angle of attack increases but it decreases when load relief control is employed. Acceleration response of load relief controller is also found to be a lower value compared to attitude controller in both positive and negative wind gust cases. Angle of attack reduction is about 30 % and acceleration value reduces about 35%.

Fig. 12 Bode magnitude plot showing aerodynamic load reduction
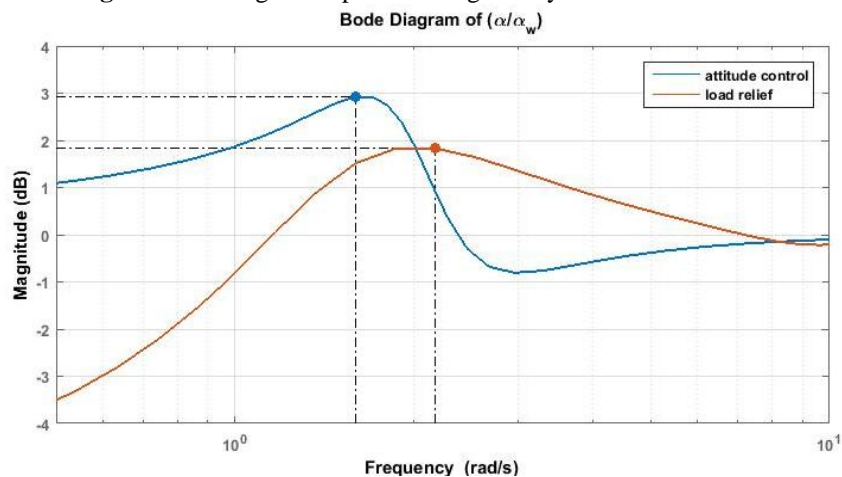
Bode magnitude plot of $\dfrac{\alpha}{\alpha_w}$ can also be analysed to check for aerodynamic load reduction. Peak magnitude of bode plot is 2.92 with attitude control and 1.83 with load relief control as shown in Fig. 12. Thus the aerodynamic load reduction achieved with load relief controller is about 35%.

V. Conclusions

The load relief control system based on acceleration feedback is studied in this paper. Attitude control gains are designed for entire flight time and load relief control gains based on acceleration feedback are designed for the high dynamic pressure period considering the rigid body dynamics. Flexible dynamics is introduced and suitable filters are designed. The designed system is found to satisfy required margins at all time instants. The system performance is examined by applying a unit step reference attitude and wind gust. From the results, it is clear that trajectory dispersion is more when load relief control is enabled but significant load reduction is achieved in presence of wind. Thus load relief control can be attempted during specific flight period,where the loads exceeds the allowable limit. As a future work, load relief controller can be analysed by replacing aerodynamic load with a wind profile to get the real time effectiveness of the designed controller and propellant sloshing can also be included in launch vehicle dynamics.

References

[1]   H. H. Burke, Aerodynamics load reduction techniques for large elastic launch vehicle, *IEEE Transactions on Automatic Control, 9(4)*, 1964, 565–569.

[2]   A. L. Greensite, *Analysis and design of space vehicle flight control systems* (Spartan Books, Washington, 1967).

[3]   J. M. Livingston and J. R. Redus, Load reducing flight control systems for the Saturn V with various payloads, *AIAA guidance, control, and flight dynamic conference*, 1968.

[4]   W. J. Klenk, An adaptive system for load relief and accurate control of launch vehicles, *AIAA 1st Annual Meeting*, 1964.

[5]   R. S. Ryan, D. K. Mowery, and S. W. Winder, Fundamental concepts of structural loading and load relief techniques for the space shuttle, *NASA technical report*, 1972.

[6]   J. H. Blackstone, Current design technology of attitude control systems for large launch vehicles, *AIAA guidance, control, and flight dynamics conference*, 1968.

[7]   N. V. Kadam, Practical design of flight control systems: Some problems and their solutions, *Defence Science Journal, 55(3)*, 2005, 211–221.